Solid Freeform Fabrication 2017: Proceedings of the 28th Annual International Solid Freeform Fabrication Symposium – An Additive Manufacturing Conference
Reviewed Paper

Design and Fabrication of Functionally Graded Material from Ti to γ-TiAl by Laser Metal Deposition

Xueyang Chen[1], Lei Yan[1], Joe Newkirk[2], and Frank Liou[1]

[1]Department of Mechanical and Aerospace Engineering,
[2]Department of Materials Science and Engineering,
Missouri University of Science and Technology, Rolla, MO 65409

Abstract

Functionally graded material (FGM) is one kind of advanced material characterized by a gradual change in properties as the position varies. The spatial variation of compositional and microstructure over volume is aimed to control corresponding functional properties. In this research, when 100% γ-TiAl was directly deposited on pure Ti substrate, cracks were formed within the γ-TiAl layer. Then a six-layer crack-free functionally graded material of Ti/TiAl was designed and fabricated by laser metal deposition (LMD) method, with composition changing from pure Ti on one side to 100% γ-TiAl on the other side. The fabricated FGM was characterized for material properties by a variety of techniques. The chemical compositions, microstructure, phases, and hardness of the composite were characterized by Scanning Electronic Microscope (SEM), Optical Microscope (OM), Energy Dispersive X-ray Spectroscopy (EDS), and hardness testing. The microstructure and chemical compositions in different layers were studied.

1. Introduction

The origin of functionally graded material (FGM) is from the National Aerospace Laboratory of Japan in 1984 during a spaceplane project. The proposed thermal barrier material is capable of withstanding a surface temperature of 2000 K and a temperature gradient of 1000 K across a 10 mm section [1]. FGM is one kind of advanced material characterized by a gradual change in properties as the position varies. The spatial variation of compositional and microstructure over volume is aimed at controlling corresponding functional properties, such as mechanical properties, thermal properties, electrical properties, etc. In FGM research, various methods to prepare and fabricate FGM materials are available. The fabrication methods include powder metallurgy [2], [3], thermal spraying [4] [5], additive manufacturing [6], [7]. Additive manufacturing is a manufacturing method that can create 3D objects. This method allows you to produce complex products with minimal lead times directly from the 3D CAD models by adding layers of materials on top of each other. The bind layers schematic could mix elemental powders of variable ratios in separate layers to fabricate FGM parts with controllable gradients, no matter the complexity [8].

There is a wide range of applications for FGM and different types of FGMs could be used in different areas of application. In aerospace and automotive area, the space shuttle utilized the FGM material made of ceramic and metal that can provide the thermal protection and load carrying capability to replace the ceramic tiles that easily to crack [9]. FGMs are also used as dental implants in the biomedical area [10], vehicle armor in defense area [11], high-density magnetic recording media in optical applications [9], cutting tools in the industry [12] etc.

Actually, compressors and turbine disks are two of the most significant parts in the aerospace industry. Turbine disks require different material properties at different regions. The rim region suffers from high temperature, requires good oxidation resistance. The core region has a relatively low temperature but requires high strength. The rim and the core have different requirements. The current approach is to use different treated nickel-based superalloys for each part. Nickel-based alloys are widely used in jet engines because it could withstand high-temperatures. In aerospace applications, Ti has a combination of excellent properties but has limitation for oxidation resistance. While, intermetallic titanium alloys such as γ-TiAl, Ti_3Al can have higher oxidation resistance and both of the two alloys can be used under high temperature. Because the density for the γ-TiAl is much lower than the nickel-based superalloys and its specific properties, γ-TiAl tends to replace them. In this way, the rim can be made of Ti_3Al or γ-TiAl, which have good high-temperature properties. And the core can be made of Ti with good strength at relatively low temperatures. However, there are some problems to join them effectively. Thus, the aim of this project is to manufacture Ti/γ-TiAl functionally gradient material (FGM) using Laser Metal Deposition (LMD) method. LMD is one of the advanced additive manufacturing technologies. It could fabricate complex near net shape metallic parts layer by layer directly from computer-aided design (CAD) models. This technique could reduce cost by reducing the buy-to-fly ratio and lead time of production.

The main goals of this work involved studying the microstructure and mechanical properties of the fabricated alloys. In this study, commercially purified (CP) titanium plate was used as the substrate material for all the depositions. The powder material was fabricated as thin wall depositions and characterized for material properties using optical and Scanning Electron Microscope (SEM) microstructure characterization, hardness testing, Energy Dispersive X-ray Spectroscopy (EDS). The study investigated the material properties of γ-TiAl manufactured by LMD method. And it showed the possibility to control properties and crack formation in the deposits. Also, it demonstrated the approach to build a complex FGM system (Ti + γ-TiAl and/or any intermediate FGM materials in between) by LMD method with hope to move to more exotic material compositions in the future.

2. Materials and Methods

2.1 Material Preparation

Under the current study, commercially purified gas atomized γ-TiAl (Ti-48Al-2Cr-2Nb) powder and pure Ti powder were used as precursor materials. For this kind of γ-TiAl powder, the addition of Cr element can increase the ductility of the material. The addition of Nb element is to enhance the oxidation resistance. Blends of the two kinds of powder with different composition were made to achieve layers in functionally graded materials (FGM). The particle size distributions of γ-TiAl and Ti powder are listed in Table 1 and Table 2 individually. The chemical compositions of the two kinds of powder are given in Table 3 and Table 4. Commercially purified (CP) titanium plate was used as the substrate material for these depositions, and substrates were prepared to the dimensions of 2 × 0.5 × 0.25 in.

Table 1. Particle size distribution of Ti-48Al-2Cr-2Nb powder (% Under).

Particle Size (μm)	150	106	75	63	53	Apparent Density (g/cc)
By Mass	99.9	66.2	25.5	14.7	4.0	2.20

Table 2. Particle size distribution of Ti powder (% Under).

Particle Size (μm)	150	53	Apparent Density (g/cc)
By Mass	98.9	0.9	2.64

Table 3. Chemical analysis of Ti-48Al-2Cr-2Nb powder (wt.%).

Elements	Ti	Al	Cr	Nb	Fe	Si	C	O
Measured	Balance	34.4	2.38	4.75	0.04	0.016	0.014	0.128

Table 4. Chemical analysis of Ti powder (wt.%).

Elements	Ti	C	O	N	H	Fe	Other
Measured	Balance	<0.01	<0.16	<0.01	<0.001	<0.12	<0.4

2.2 Deposition System

In this study, a 1 kW continuous wave fiber laser with a wavelength of 1064 nm was used to deposit the elemental powder blends. A melt pool spot size of approximately 2 mm was obtained through a lens of 750 mm focal length. A ceramic tube nozzle was used in conjuncture with a CNC (Computer Numerical Control) table to facilitate movement and perform deposition. Argon gas was used to implement an inert atmosphere and was also used as a carrier gas to deliver the powder mixture to the melt pool.

The schematic layout of the LMD system is shown in Figure 1. LMD deposition is an additive manufacturing technique capable of fabricating complicated structures with superior properties [13]. The applications of this technique include coatings, rapid prototyping, tooling, repair, etc. LMD uses a focused laser beam as a heat source to create a melt pool into which powder feedstock is injected. The powder material is metallurgically bonded to the substrate through solidification [14].

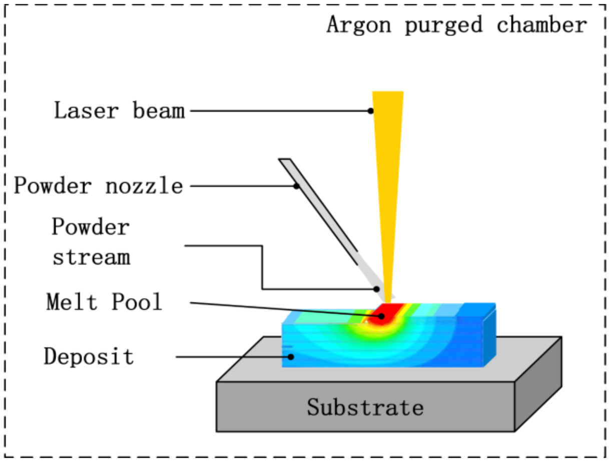

Figure 1. Schematic layout of the LMD (Laser Metal Deposition) system [15].

2.2 Experimental Procedure

In this research, three kinds of experiments have been designed in order to get crack-free Ti/γ-TiAl deposit.

In the first kind of experiment, set-up 1 has been used to deposit Ti-48Al-2Cr-2Nb powder on CP Ti substrate directly, as Figure 2 (a) showed below. In this set-up, the substrates were directly connected with the fixture. Thin wall depositions were fabricated by performing single melt pool layer by layer. Before deposition, a preheat scan of running the laser across the substrate surface at 1 kW power without powder was performed, in order to ensure perfect bonding. The preheating process was also used to heat up the substrate and rid the surface of the substrate from oxide scale buildup, surface impurities, and, surface imperfections. Laser transverse speed was set at 600 mm/min for all the depositions. The laser power was set at 600 W. The initial 2 layers of deposition carried out a duty cycle of 100% to ensure perfect bonding with the substrate. The next 4 layers keep the duty cycle of 80% and then drop to 60% for another 4 layers. The rest of the deposition was carried at a duty cycle of 40%. The actual laser power is calculated by multiplying the laser power by the duty cycle. The same deposition scheme and parameters were used for all the depositions. This was expected to ensure an unbiased comparison between different depositions. The second kind of experimental design used the set-up 2 as shown in Figure 2 (b). The insulating refractory bricks were inserted between the substrate and the fixture.

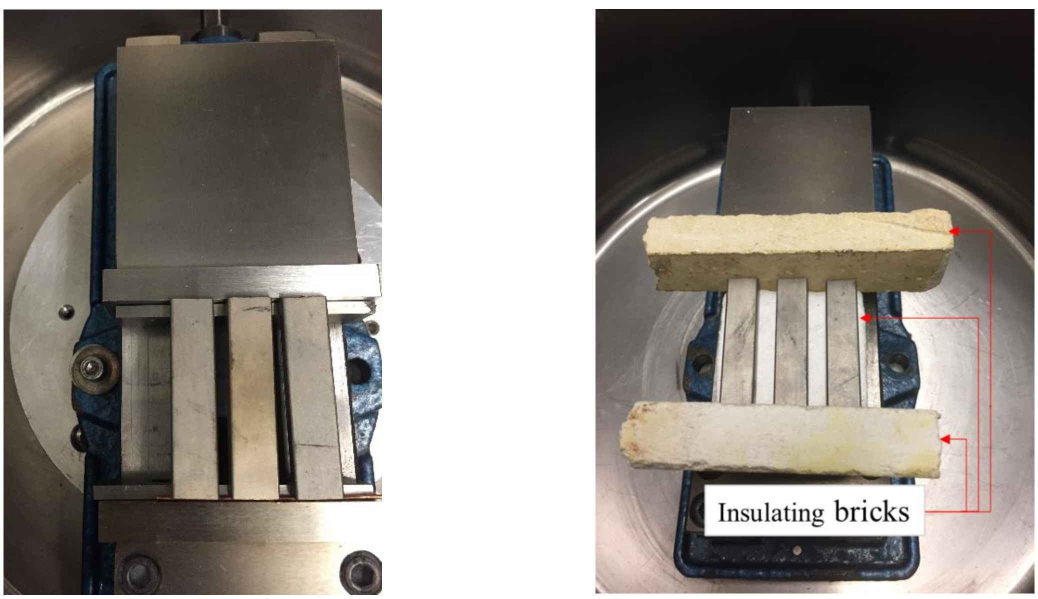

(a) Set-up 1 (b)Set-up 2

Figure 2. Two experimental set-ups

The third experimental design was used to manufacture the crack-free functionally gradient material (FGM) from Ti to γ-TiAl. The FGM study included material design, material preparation, and evaluation of material properties. The FGM path was developed as shown in Figure 3. The atomic percentage of each element and possible phase composition of every layer in the FGM deposit are also listed in Table 5. Powders were weighed for desired compositions in a glove box under an argon atmosphere and sealed in bottles before starting the deposition process. In this study, γ-TiAl powder and pure Ti powder were used. The as-blended powder mixtures can be used to form the layers in the functionally graded materials. These bottles were then shaken using a Turbula® mixer (Glen Mills Inc., Maywood, NJ, United States) for 20 min to obtain thorough mixing and homogeneity within the powder blends. During the process, there is no insulating brick used here by taking use of the first experimental set-up (set-up 1).

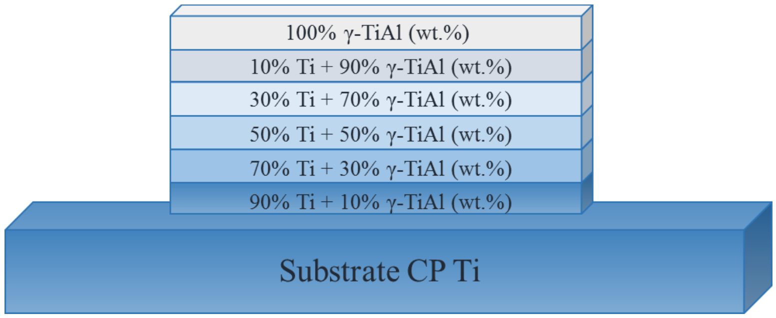

Figure 3. The designed functionally graded material (FGM) path

Table 5. Particle size distribution of Ti-48Al-2Cr-2Nb powder (% Under).

Weight Percentage	Ti at.%	Al at.%	Cr/Nb at.%	Possible Phase Composition
100% γ-TiAl	48.00	48.00	2.00	$\alpha_2 + \gamma$
10% Ti + 90% γ-TiAl	52.30	44.03	1.83	$\alpha_2 + \gamma$
30% Ti + 70% γ-TiAl	61.40	35.63	1.48	$\alpha_2 + \gamma$
50% Ti + 50% γ-TiAl	71.28	26.51	1.10	α_2
70% Ti + 30% γ-TiAl	82.01	16.60	0.69	$\alpha_2 + \alpha$
90% Ti + 10% γ-TiAl	93.73	5.79	0.24	α

After deposition, vertical transverse sections were cut using a wire Electro-Discharge Machine (wire-EDM, Hansvedt Industries Inc., Rantoul, IL, United States) and mounted in Bakelite for grinding and polishing. Kroll's reagent containing 30 ml H_20, 10ml HNO_3, and 10 ml HF was used for etching the samples. Hirox optical microscope was used to perform microstructure imaging. Helios Nanolab 600 SEM (FEI Company, Hillsboro, OR, United States) equipped with an Oxford Energy Dispersive Spectrometer was used to get the chemical compositions. The Vickers hardness measurements were performed using a Struers Duramin micro-hardness tester (Struers Inc., Cleveland, OH, United States). Press load of 9.81 N and load time of 10 s were used during the hardness tests.

3. Results and discussion

3.1 Deposit Profile

Figure 4 shows the deposited samples in the first experimental design. The image of the γ-TiAl deposit made by using set-up 1 in the first design has been shown in Figure 4 (a). It could be seen that there are some cracks in the deposit. Then with the same setup, another deposited sample was made from the powder blend of 80 wt.% γ-TiAl +20 wt.% Ti. Figure 4 (b) demonstrates the 80 wt.% γ-TiAl +20 wt.% Ti sample deposited by using set-up 1. It has been found that it is possible to make crack-free deposits with the blend. It is theorized that the cracks that mainly exist in the vertical direction are caused by residual stress. It is known that there exists a great difference in the thermal expansion coefficient between Ti and γ-TiAl. Ti has the thermal expansion coefficient of $8.9 \times 10^{-6} K^{-1}$, while γ-TiAl shows $14.4 \times 10^{-6} K^{-1}$. Due to the high residual thermal stresses between the Ti and γ-TiAl layers, it would result cracks during the cooling process after deposition. However, the layer of Ti + γ-TiAl deposits could play a role in reducing the interfacial residual thermal stresses. Therefore it could cause some cracks in the deposit by directly depositing γ-TiAl powder on Ti substrate, however crack-free γ-TiAl deposit could be made on the Ti substrate by using the powder blend of γ-TiAl and 20 wt.% Ti.

(a) γ-TiAl sample without insulating bricks

(b) 80 wt.% γ-TiAl +20 wt.% Ti sample without insulating bricks

Figure 4. Deposited samples in the first experimental design

Then in order to get a crack-free γ-TiAl deposit, the set-up 2 has been used in the second experimental design, as shown in Figure 2 (b). The image of the γ-TiAl deposit made by using set-up 2 has been shown in Figure 5. It has been found that the deposited sample has no cracks. In this set-up, the insulating bricks were inserted between the substrate and the fixture. Because these materials thermally isolate the substrate, the bricks could retain more of the input laser energy and decrease cooling rate. Then many conditions, such as boundary conditions, thermal insulation, and post-process heat treatment, may affect the mechanical properties of deposits.

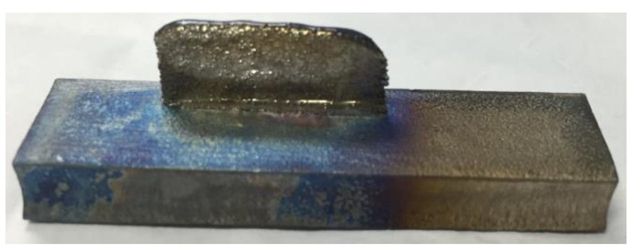

Figure 5. Deposited sample in the second experimental design

However, it is not very flexible to fabricate some big and complex parts with insulating bricks in the industry area. It is necessary to develop a gradient path to realize the same target of depositing crack-free γ-TiAl deposit on Ti substrate. Then an FGM path has been designed, as shown in Figure 3. The objective of the designed FGM is to meet the expected requirements by eliminating the obvious interface between composite materials in different layers, just the same as bones, teeth, etc. in nature. Also, the FGM is also designed to accommodate materials for specific applications. During the FGM deposition process, there was no insulating brick used. From Figure 3, the FGM parts were made with five different powder blends and the top layer is 100% γ-TiAl. Along the deposit, there are six regions with different chemical composition. The gradients between different layers could smooth transition to reduce the opportunity of failure. The transient layer of Ti + γ-TiAl deposits could gradually reduce the residual thermal stresses. Figure 6 showed the image of the FGM deposit and its transverse section after cutting.

(a) FGM sample

(b) Transverse section of the FGM deposit

Figure 6. Deposited sample in the FGM design

3.2 Vickers hardness

Figure 7 shows the Vickers hardness distribution of the deposited samples without using insulating bricks in the first experimental design. By applying post heat treatment during the deposition process, the Vickers hardness values of the deposits could also be compared in this Figure. It was observed that the Vickers hardness values of the γ-TiAl layers varied around 375 HV in the middle part of the deposit zone, then increased to 450 HV as it progressed into the top of the deposit. While the deposit by using the powder blends of 80 wt.% γ-TiAl +20 wt.% Ti had a Vickers hardness of around 420 HV. The literature reported γ-TiAl Vickers hardness was 425 HV. And when comparing the two kinds of deposits under different conditions of performing post heat treatment or not, it has been found that the post heat treatment on deposit would increase the hardness values, but could not make significant changes.

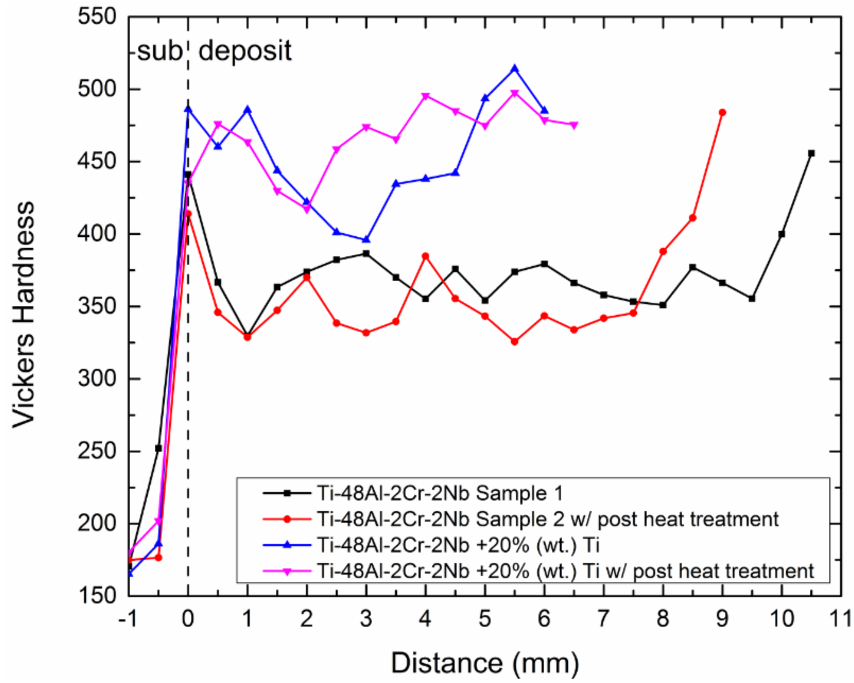

Figure 7. Vickers hardness distribution of the deposited samples in the first experimental design.

Figure 8 shows the hardness distribution of the deposited samples under different laser power with using insulating bricks in the second experimental design. It can be observed that when other parameters stayed the same, the higher the laser power, the lower the Vickers hardness. The reason should be the increase of the energy input. It would decrease the cooling rate, and then cause coarser microstructure and get lower hardness values. Therefore with insulating bricks to decrease the cooling rate, it is much easier to get crack-free γ-TiAl deposits.

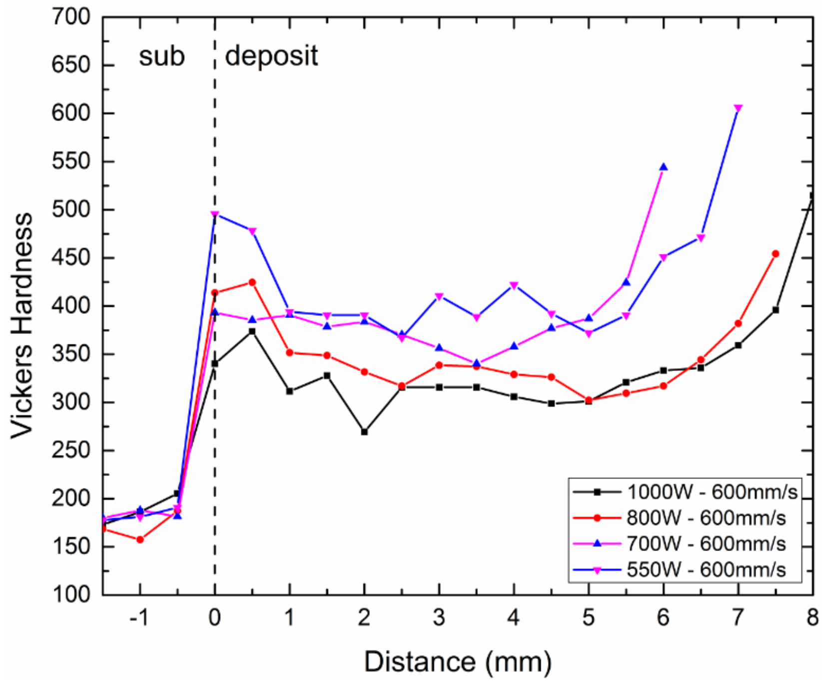

Figure 8. Vickers hardness distribution of the deposited samples in the second experimental design.

Functionally graded materials (FGM) is one kind of advanced material. They have a gradual change in properties as the position varies. As shown in this Figure 3, the volume fraction of one material will change from 100% on one side to zero on another side, and another constituent will change in the other way around. Their composition and microstructure vary in space by following a predetermined law. This change also leads to a gradient of properties and performance, such as mechanical properties, thermal properties. Figure 9 shows the Vickers hardness distribution of the FGM sample. The 100% TiAl layer is harder than previous composition layers.

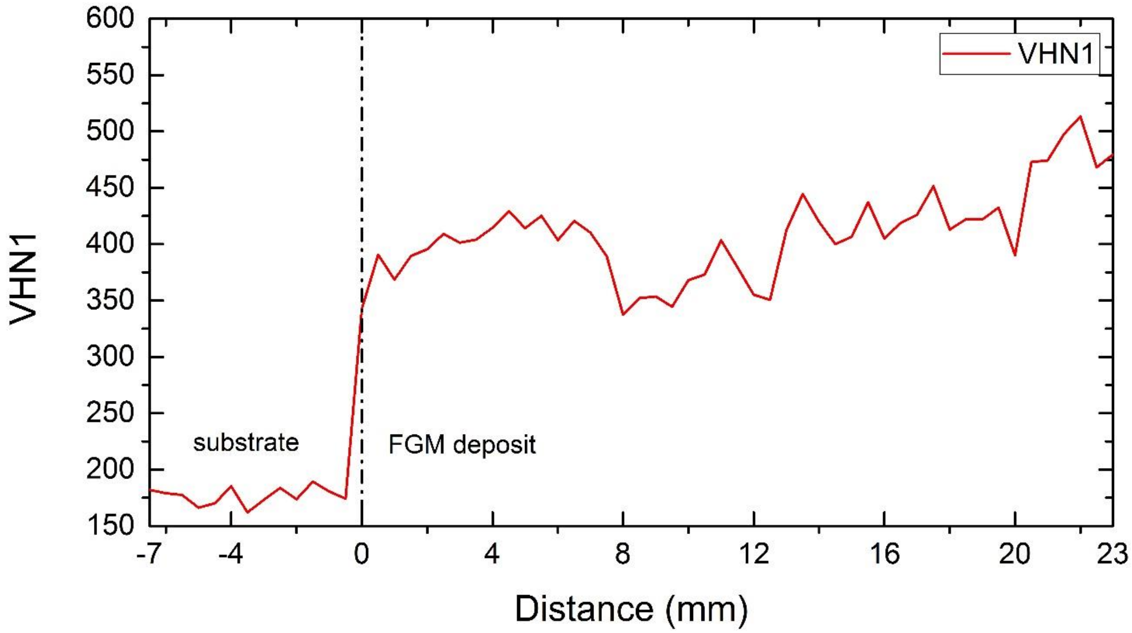

Figure 9. Vickers hardness distribution of the FGM sample

3.3 Microstructure & EDS test

The microstructures of γ-TiAl deposits from Set-up 1 and Set-up 2 are shown in Figure 10. It shows that most prevalent microstructure for both is lamellar.

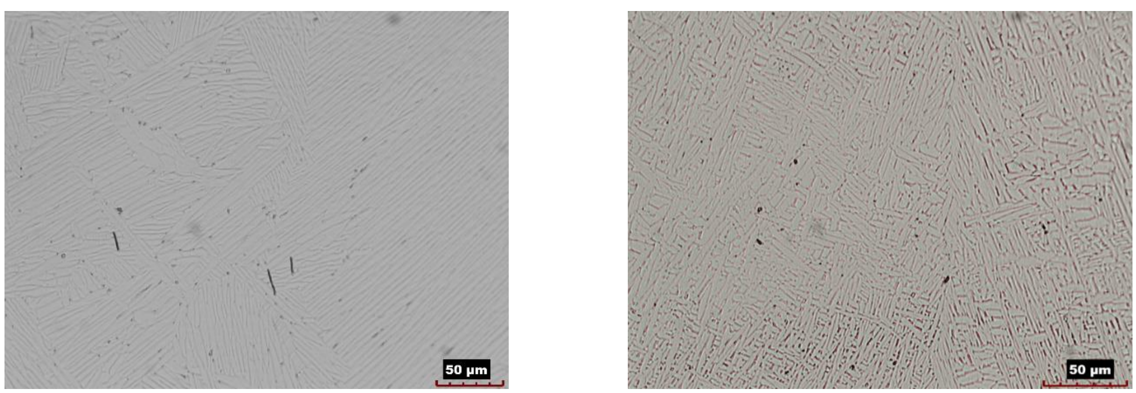

(a) Microstructure of the γ-TiAl from set-up 1 (b) Microstructure of the γ-TiAl from set-up 2

Figure 10. Microstructures of the γ-TiAl from two set-ups

And Figure 11 shows the EDS result of the FGM deposit. Line scan was performed along the deposit, it differentiated six regions with different compositions listed in Table 5. The designed length for each region is 5 mm. Region height difference can be attributed to the powder capture efficiency.

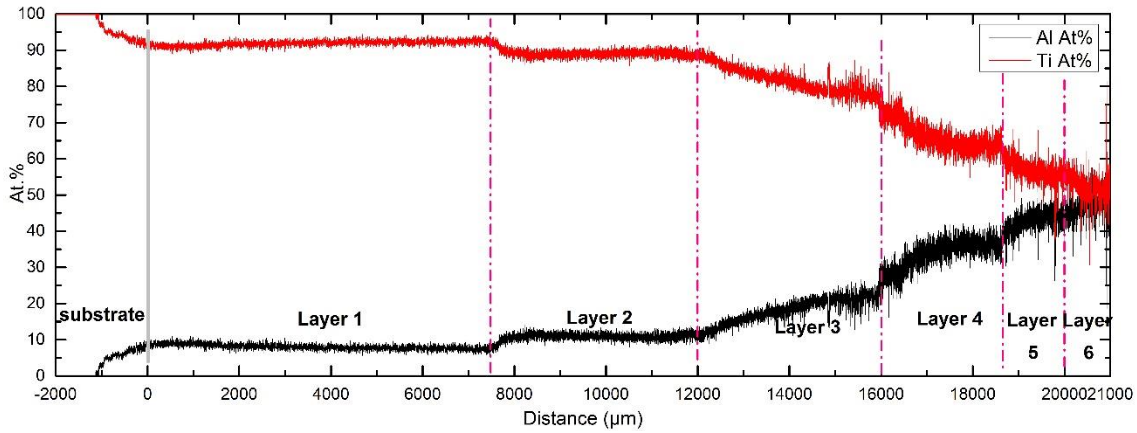

Figure 11. EDS result of the FGM deposit

4. Conclusions

The current research was implemented to investigate the feasibility of combining Ti with γ-TiAl via the LMD process. The fabricated material was characterized using techniques such as scanning electron microscopy, hardness testing, EDS. The conclusions from the analyses include:

- Crack-free γ-TiAl deposits could be fabricated by using insulating bricks to control the cooling rate during LMD process.
- Proposed an FGM path to successfully join titanium alloy with γ-TiAl.
- Mechanical properties of γ-TiAl would be affected by are affected by processing parameter. Increasing energy input would decrease the cooling rate and decrease the Vickers hardness.
- The microstructure in the γ-TiAl deposit is lamella.

5. Acknowledgements

This project was supported by The Boeing Company through the Center for Aerospace Manufacturing Technologies (CAMT). Their financial support is greatly appreciated.

6. References

[1] M. KOIZUMI, “FGM ACTIVITIES IN JAPAN,” *Compos Part B Eng*, vol. 28, pp. 1–4, 1997.
[2] a. Shahrjerdi, F. Mustapha, M. Bayat, S. M. Sapuan, and D. L. a. Majid, “Fabrication of functionally graded Hydroxyapatite- Titanium by applying optimal sintering procedure and powder metallurgy,” *Int. J. Phys. Sci.*, vol. 6, no. 9, pp. 2258–2267, 2011.
[3] F. Thummler and R. Oberacker, *Introduction to Powder Metallurgy*, vol. 34, no. 3. 1995.
[4] V. Cannillo, L. Lusvarghi, T. Manfredini, M. Montorsi, C. Siligardi, and A. Sola, “Glass-ceramic functionally graded materials produced with different methods,” *J. Eur. Ceram. Soc.*, vol. 27, no. 2–3, pp. 1293–1298, 2007.

[5] M. Belmonte, J. Gonzalez-Julian, P. Miranzo, and M. I. Osendi, “Continuous in situ functionally graded silicon nitride materials,” *Acta Mater.*, vol. 57, no. 9, pp. 2607–2612, 2009.
[6] T. Durejko, M. Zietala, W. Polkowski, and T. Czujko, “Thin wall tubes with Fe3Al/SS316L graded structure obtained by using laser engineered net shaping technology,” *Mater. Des.*, vol. 63, pp. 766–774, 2014.
[7] H. S. Ren, X. J. Tian, and H. M. Wang, “Effect of heat treatment on microstructure and mechanical properties of a graded structural material,” *Mater. Sci. Eng. A*, vol. 614, pp. 207–213, 2014.
[8] M. S. El-Wazery and A. R. El-Desouky, “A review on functionally graded ceramic-metal materials,” *J. Mater. Environ. Sci.*, vol. 6, no. 5, pp. 1369–1376, 2015.
[9] A. Saiyathibrahim, S. S. Mohamed Nazirudeen, and P. Dhanapal, “Processing Techniques of Functionally Graded Materials - A Review,” *Proc. Int. Conf. Syst. Sci. Control. Eng. Technol.*, vol. 1, pp. 98–105, 2015.
[10] A. Tampieri, G. Celotti, S. Sprio, A. Delcogliano, and S. Franzese, “Porosity-graded hydroxyapatite ceramics to replace natural bone,” *Biomaterials*, vol. 22, no. 11, pp. 1365–1370, 2001.
[11] Y. M. Soon, K. H. Shin, Y. H. Koh, J. H. Lee, W. Y. Choi, and H. E. Kim, “Fabrication and compressive strength of porous hydroxyapatite scaffolds with a functionally graded core/shell structure,” *J. Eur. Ceram. Soc.*, vol. 31, no. 1–2, pp. 13–18, 2011.
[12] Y. Miyamoto, W. A. Kaysser, B. H. Rabin, A. Kawasaki, and R. G. Ford, “Functionally Graded Materials: Design, Processing and Applications,” in *Kluwer Academic*, 1999.
[13] X. Chen, L. Yan, W. Li, Z. Wang, F. Liou, and J. Newkirk, “Effect of Powder Particle Size on the Fabrication of Ti-6Al-4V Using Direct Laser Metal Deposition from Elemental Powder Mixture,” vol. 6, pp. 348–355, 2016.
[14] X. Chen, L. Yan, S. Karnati, Y. Zhang, and F. Liou, “Fabrication and Characterization of AlxCoFeNiCu1−x High Entropy Alloys by Laser Metal Deposition,” *Coatings*, vol. 7, no. 4, 2017.
[15] X. Chen, L. Yan, W. Li, F. Liou, and J. Newkirk, “Effect of Powder Particle Size on the Fabrication of Ti-6Al-4V using Direct Laser Metal Deposition from Elemental Powder Mixture,” pp. 714–722, 2016.